Editorial Manager(tm) for Analog Integrated Circuits and Signal Processing
Manuscript Draft

Manuscript Number: ALOG618

Title: LINEAR ANALYSIS OF THE INFLUENCE OF FIR FEEDBACK FILTERS ON THE RESPONSE OF THE PULSED DIGITAL OSCILLATOR

Article Type: DTIP2006

Keywords: pulsed digital oscillators; MEMS-based circuits; sampled feedback structures

Corresponding Author: Dr. Manuel Dominguez, Ph.D.

Corresponding Author's Institution: Technical University of Catalonia (UPC)

First Author: Manuel Dominguez, Ph.D.

Order of Authors: Manuel Dominguez, Ph.D.; Joan Pons-Nin, Ph.D.; Jordi Ricart; Jérôme Juillard, Ph.D.; Éric Colinet

LINEAR ANALYSIS OF THE INFLUENCE OF FIR FEEDBACK FILTERS ON THE RESPONSE OF THE PULSED DIGITAL OSCILLATOR

M. Domínguez[1], J. Pons[1], J. Ricart[1], J. Juillard[2], E. Colinet[2]

[1]MNT, Universitat Politècnica de Catalunya. Barcelona, Spain.

[2] Département Traitement du Signal & Systèmes Électroniques, SUPELEC. France.

ABSTRACT

The objective of this work is to extend the linear analysis of Pulsed Digital Oscillators to those topologies having a Finite Impulse Response (FIR) in the feedback loop of the circuit. It will be shown with two specific examples how the overall response of the oscillator can be adjusted to some point by changing the feedback filter, when the resonator presents heavy damping losses. Extensive discrete-time simulations and experimental results obtained with a MEMS cantilever with thermoelectric actuation and piezoresistive position sensing are presented. It will be experimentally shown that the performance of the oscillator is good even below the Nyquist limit.

1. INTRODUCTION

The use of resonant MEMS devices working near their resonance is widely extended today to a growing number of applications, which include RF components, chemical and gas sensors, accelerometers, gyroscopes, actuators, etc. MEMS resonators are an attractive option to fix the oscillation frequency in such applications because of their high quality and frequency stability properties. However, most actuation schemes for MEMS (electrostatic, thermoelectric, etc.) are non-linear and therefore the design of large-signal oscillators is not simple. In this way, several oscillator topologies have been proposed in the past; most of them linearize the response of the MEMS by applying a suitable bias voltage and therefore the displacement of the resonator is in the small signal range. On the other hand, large-signal oscillators proposed in the literature exhibited chaotic behavior [1].

The Pulsed Digital Oscillator (PDO) [2,3] is a set of sigma-delta based topologies for MEMS that was originally proposed by the authors to overcome these difficulties so that non-chaotic oscillation waveforms can be obtained even working in the large signal range.

This work is an extension of [4,5] and introduces and analyzes two new feedback loop structures for the PDO, called *double feedback*. The goals of this new architecture are to adjust the overall response of the PDO when the resonator has high damping losses. To this effect, the main features of the classical, or *single feedback*, PDO architecture are reviewed in section 2, whereas section 3 introduces the *double feedback* structures and compares them to the classical one through simulations. Finally, section 4 extends this comparison with experimental results.

2. PDO FUNDAMENTALS

2.1. Architecture and key features

The classical PDO architecture is depicted in Figure 1. We can see that it has a simple and relatively easy to implement structure which includes the MEMS device plus a feedback actuation loop composed by a sign detector, a variable number of delay blocks and an amplifier. Some key features of the PDO are:

a) Very short pulses (i.e. deltas) of force of constant amplitude F are supplied to the resonator. This actuation scheme avoids the above mentioned non-linearities present in MEMS actuation and has been analyzed and extended in a recent work [6] to other MEMS-based applications such as an accelerometer system.

b) The PDO is a sampled circuit and, assuming a typical two-parallel plate MEMS resonator structure, at each sampling time it is only checked if the moveable plate is above or below its 'zero', or rest, position. Such simple position measurement requirements enormously simplify the design and implementation of the MEMS device and of the circuit needed to manage the feedback signal.

c) The PDO is a digital oscillator and, in over-sampling conditions, the oscillation frequency (f_{OSC}) is directly extracted from the spectrum of the bit stream at the output of the sign detector.

d) The PDO exhibits 'perfect' sinusoidal oscillations at the natural frequency of the resonator (f_0) for certain sampling frequency (f_S) sets [3]. It has also been demonstrated that the energy transfer from the electrical domain to the mechanical one is maximized in such 'perfect' sample frequencies.

e) When the damping losses in the MEMS resonator are relevant, and due to the presence of the 1-bit quantizer in the feedback loop, the oscillation frequency (f_{OSC}) as a function of the sampling ratio (f_0/f_S) exhibits a fractal shape [2,3], which looks rather similar to a distorted version of the well-known devil's staircase fractal [7]. This effect has also been recently reported for a very similar circuit topology in [6].

f) It has been recently demonstrated that the PDO can also work very well with sample frequencies below the Nyquist limit [8]. However, with this extension to higher frequency ranges the effects of the damping losses mentioned above become more important, especially when working in deep under-sampling conditions.

2.2. Basic PDO theory

Let us now focus in the PDO structure shown in Figure 1 (for m=1), hereafter called *single feedback*. By assuming a typical 1D mass-spring-damping model for the parallel-plate MEMS resonator [9] and applying a linear analysis, it can be easily obtained that the structure produces the following normalized digital oscillation frequency [2,3],

$$f_D = \frac{1}{2\pi}\cos^{-1}\left(e^{-\rho 2\pi f_0/f_S}\cos\left(2\pi\frac{f_0}{f_S}\sqrt{1-\rho^2}\right)\right) \qquad (1)$$

being the digital oscillation frequency $f_{OSC}=f_D f_S$, and f_S the sampling frequency, ρ the dimensionless damping factor and f_0 the natural frequency of the MEMS resonator. These parameters are related to the well-known ones of the MEMS model according to,

$$\rho = \frac{b}{2\sqrt{km}} \qquad \omega_0 = 2\pi f_0 = \sqrt{\frac{k}{m}} \tag{2}$$

where m is the mass of the moveable plate, k is the spring factor, or stiffness, and b is the damping factor. Extensive discrete-time simulations that have been carried out reveal that, in the presence of heavy damping losses, the PDO response becomes fractal and that f_D clearly departs from the natural frequency of the resonator, in particular for sampling frequencies close to the Nyquist limit (see Figure 2). This last effect is not only due to the presence of the fractal, but also because of the tendency marked by equation (1).

3. GENERAL DOUBLE FEEDBACK TOPOLOGY

As it has been mentioned above, the resonator damping losses present a two-fold non-desired effect. First, the response of the oscillator becomes fractal, and second the oscillation frequency can depart from the natural frequency of the resonator. This second effect can be observed in Figure 2. In order to obtain a reduction of the influence of the damping losses on the PDO performance, a review of the linear analysis which led to equation (1) has been carried out. From this point of view it can be concluded that such reduction could be obtained by adding some digital filtering in the feedback loop. Two different feedback topologies have been proposed in [4,5]. These topologies can be seen in Figure 3 (the one proposed in [4] is with δ=1 and that of [5] is with δ=-1.

The linear analysis of the circuit assumes that the quantization noise samples at the output of the comparator are independent and have a uniform distribution. This is of course not rigorous but it is possible with this approximation to obtain good estimates of the non-linear response of the oscillator, as a function of the sampling frequency and the damping losses of the resonator.

The z-transform of impulse response of the MEMS resonator, considering a 1-D model for a given sampling frequency (f_S), is:

$$H(z) = \frac{K_n \, z^{-1}}{1 - \alpha z^{-1} + \beta z^{-2}} \tag{3}$$

where:

$$\begin{aligned} K_n &= \frac{e^{-\rho\omega_0 T_S} \sin(\omega_0 T_S \sqrt{1-\rho^2})}{m\omega_0\sqrt{1-\rho^2}} \\ \alpha &= 2e^{-\rho\omega_0 T_S} \cos(\omega_0 T_S \sqrt{1-\rho^2}) \\ \beta &= e^{-2\rho\omega_0 T_S} \end{aligned} \tag{4}$$

where $T_S=1/f_S$ is the sampling period. Now, the characteristic equation of the oscillator is:

$$1 - (\alpha - FK_n)z^{-1} + (\beta + \delta FK_n)z^{-2} \tag{5}$$

By adjusting the value of F to $(1-\beta)/K_n$ it is possible to force an oscillation in the circuit, following the linear analysis

approximation. The resulting oscillation frequency is $f_D f_S$, where f_D is called the normalized digital oscillation frequency, which is given by the following expression [9],

$$f_D = \frac{1}{2\pi}\cos^{-1}\left(e^{-\rho\omega_0 T_S}\cos(2\pi\frac{f_0}{f_S}\sqrt{1-\rho^2}) + \frac{\delta}{2}\left(e^{-2\rho\omega_0 T_S}-1\right)\right) \quad (6)$$

It is remarkable that although linear theory requires that F is given a specific value, the presence of the comparator in the actual PDO makes it no longer necessary. It is only an amplification factor whose effect is cancel out by the comparator. On the other hand, with this structure the force pulses applied to the MEMS can take up to three different values {+2F, +F, 0}, for δ=1, and {+F,0,-F}, for δ=-1, instead of the two possible values {+F, 0} which are possible with the single feedback architecture. This would represent in principle a difficulty because one of the main advantages of PDO circuits is their simple actuation scheme (short pulses of force, all of the same amplitude), which sheds protection against some non-linearities in actuation usually found in MEMS devices. As it will be shown later, in Section 4, this can be easily overcome by applying pulses of different duration.

One can also follow the lines described in [5] in order to make the analysis of both systems. As opposed to the linear approach described above, this approach is exact; however it does not yield, in the present case, analytical expressions of the oscillation frequency. However, it does yield rigorous bounds on the value of the pulsation of mixed-signal relay feedback systems. This is illustrated in Figure 4. One can see that, for large oversampling ratios, the PDO with δ=-1 oscillates at a pulsation closer to the natural pulsation of the system and that the steps in the frequency response become very small. On the hand, as the oversampling ratio drops, the steps become much larger for the δ=-1 system, whereas they stay roughly the same size for the δ=1 system.

Discrete-time simulation results of the double feedback PDOs obtained for a resonator with ρ=0.005 are shown in Figure 5. After a comparison of the results of Figures 2 and 5, it can be concluded that the double feedback approach produces a wider range of oscillation frequencies which are closer to the natural frequency of the resonator for different regions than in the single feedback case, even in presence of heavy damping losses. In particular, the sample ratio values around the Nyquist limit ($f_0/f_S=1/2$) produce results similar to the 'no-losses' ($\rho=0$) case, if δ=1, and near $f_0/f_S=1$ the topology with δ=-1 provides a better result. It is important to notice, though, that the fractal behaviour still remains, but becomes more evident for the deep over-sampling and deep undersampling ranges.

4. EXPERIMENTAL RESULTS

The promising perspectives provided by the double feedback architecture about a reduction of the effects of the damping losses on the oscillator performance for some frequency ranges have been checked in a first set of experimental measurements.

4.1. Measurements setup

The measurements setup (see Figure 6) is basically the same one that was used in recent works [2,8] but with the changes in the digital section needed to implement and select between a single and a double feedback loop. The MEMS

resonator comes from the same batch previously described in [2] and it is a cantilever with thermoelectric actuation and piezoresistive position sensing through a Wheatstone bridge. The natural frequency, measured with a vibrometer, is $f_0=93,688$ *KHz.*

Due to the thermoelectric actuation of the resonator, force pulses are short voltage pulses provided by open-drain power transistors, while the sign detector role is played by an instrumentation amplifier plus a comparator. Digital control, sampling frequency selection, single and double feedback selection, number of delays and overall timing have been implemented on an is Programmable Logic Device. The values of force {+2F, +F, 0} for the double feedback (δ=1) case are obtained by modulating the time length of the voltage pulses ({$2T_p$, T_p, 0} being T_p the standard duration of an actuation pulse). In the other case (δ=-1) {+F,0,-F} the translation produces also {$2T_p$, T_p, 0}. In order to work with non-negligible damping values, all measurements were made in air and at room temperature.

4.2. Results and discussion

Figure 7.a shows an oscilloscope screen capture of the resonator position, obtained after amplification, and the set of voltage pulses applied to the MEMS excitation transistors for a single feedback topology with *m=1* (see Figure 1) and a 'perfect' sample ratio $f_0/f_S=0,25$. Let us note that, accordingly to our previous results, an excellent and stable sinusoidal waveform and a regular series of bits of the form '110011 ...' are obtained for this case.

Figure 7.b shows the results for the same case as in Figure 7.a but for a double feedback topology with δ=1. We can see there that the MEMS input pulses follow the fixed pattern '12101210 ...' and that the resulting position waveform is the same one as in Figure 7.a but with a slight amplitude increase. Moreover, the bit stream spectrums corresponding to the single and double feedback cases look exactly the same, providing a peak value at $f_{OSC}=93,68$ *KHz*.

In good agreement with the conclusions of the previous sections, these results tell us that no significant advantages are obtained when the double feedback is applied to the sample ratio $f_0/f_S=0,25$, which corresponds to a 'perfect' frequency case when working with the single feedback structure. We can also notice that the energy efficiency in the double feedback case is poorer: it provides more energy to the MEMS than in single feedback to obtain the same output response.

Again according to the conclusions of previous section, benefits of using the double feedback scheme should be more apparent for sample ratios closer to the Nyquist limit, in the case δ=1. To this effect, measurements for a sample frequency $f_S=2,489f_0$ have been carried out. For this sampling frequency it is difficult to obtain a good waveform with the single feedback topology. On the other hand, the oscilloscope screen captures of Figure 8.a show that the double feedback structure with δ=1 exhibits a fair sinusoidal waveform, plus a stable and regular '111100111100 ...' input bit pattern for the same $f_S=2,489f_0=233KHz$ case. The corresponding analog and bit stream spectra, shown in Figures 9.a and 9.b, are also very good, with a peak value located at $f_{OSC}=93,66$ *KHz* for the bit stream spectrum.

The same set of experimental results for $f_S=2,489f_0$ but for a double feedback topology with δ=-1 have been also obtained. The MEMS position waveform can be seen in Figure 8b, together with the generated bit stream and the pulses fed into the resonator. Figure 9.c shows the spectrum of the analog position of the resonator and finally Figure 9.d shows the spectrum of the corresponding bit stream. Let us note that, as expected, the spectra look rather similar to the ones obtained for the δ=1 case.

Moreover, a closer observation of Figures 8.a and 8.b reveals that, as it could be expected, the comparator output is identical for both the δ=1 and δ=-1 cases: the stable and regular '...1010010100...' bit sequence which corresponds to the sign samples of a sinusoidal waveform with $f_S \approx 2.5 f_0$. Then, for the δ=1 case a regular '... 111100 ...' time-length input pattern is generated after the feedback loop, while a regular time-length input pattern of the form '... 20201 ...' is generated for the δ=-1 case. Let us note that these results are in good agreement with the theory shown above.

Finaly, the oscilloscope screen captures included in Figure 10 are examples of how the double feedback topologies work (Figure 10.a is for δ=1, while Figure 10.b is for δ=-1) for the undersampled and closer to the Nyquist limit case $f_S = 1{,}23 f_0 = 115KHz$. Nearly sinusoidal waveforms and fair bit stream spectra are obtained for both cases. The spectrum peaks are located around $f_{OSC} = 93{,}7\ KHz$.

5. CONCLUSIONS

Two different feedback loops for PDO structures have been introduced and analyzed. Simulation results show that the double feedback forces the oscillator to put the oscillation frequency closer to the natural frequency of the MEMS resonator, even in the case of heavy damping factors. Experimental results confirm that the double feedback architecture reduces the influence of the resonator damping losses and it also allows working in wider frequency ranges than the single feedback one.

6. REFERENCES

[1] J. Bienstman, R. Puers, J. Vandewalle, "Periodic and chaotic behaviour of the autonomous impact resonator", *Proc. of MEMS-1998*, pp. 562-567, 1998.

[2] M. Domínguez, J. Pons, J. Ricart A. Bermejo, E. Figueras, "A Novel Sigma-Delta Pulsed Digital Oscillator (PDO) for MEMS". *IEEE Sensors Journal,* Vol.5, no.6, pp.1379-1388, December 2005.

[3] M. Domínguez, J. Pons, J. Ricart, A. Bermejo, E. Figueras, M. Morata, "Analysis of the Σ-Δ Pulsed Digital Oscillator (PDO) for MEMS". *IEEE Trans on Circuits and Systems-I*, Vol.52, no.11, pp. 2286-2297, November 2005.

[4] M. Domínguez M. Dominguez, J. Pons, J. Ricart, J. Juillard, E. Colinet, "Influence of the feedback filter on the response of the Pulsed Digital Oscillator". *Proc. of the Symposium on Design, Test, Integration and Packaging of MEMS / MOEMS (DTIP 2006)*, pp. 42-46, Stresa, Lago Maggiore, Italy, April 2006.

[5] J. Juillard, E. Colinet, M. Dominguez, J. Pons, J. Ricart, "Resolution Limits for Resonant MEMS Sensors Based on Discrete Relay Feedback Techniques". *Proc. of the Symposium on Design, Test, Integration and Packaging of MEMS / MOEMS (DTIP 2006),* pp. 83-87, Stresa, Lago Maggiore, Italy, April 2006.

[6] E. Colinet, J. Juilard, S. Guessab, R. Kielbasa, "Actuation of Resonant MEMS using Short Pulsed Forces". *Sensors and Actuators phys. A*, Vol. 115, pp. 118-125, 2004.

[7] O. Feely. "A tutorial introduction to non-linear dynamics and chaos and their application to sigma-delta modulators". *Int. Circuit Theory Appl*., Vol. 25, pp. 347-367, 1997.

[8] M. Domínguez, J. Pons, J. Ricart, E. Figueras, "The MEMS Pulsed Digital Oscillator (PDO) below the Nyquist limit". Submitted to *Sensors And Actuators*, June 2006.

[9] S.D. Senturia, "Microsystem Design". *Kluwer Academic Publishers*, 2001.

FIGURE CAPTIONS

Figure 1. Block diagram of the "classic" m-delay pulsed digital oscillator (PDO).

Figure 2. Discrete-time simulation results versus linear analysis results for a single feedback PDO topology and relevant damping losses (ρ=0.05).

Figure 3. Block diagram of the double feedback PDO.

Figure 4. Upper and lower bounds of the oscillation pulsation of the two PDO schemes for different values of the oversampling ratio and ρ=0.03.

Figure 5. Discrete-time simulation results for a double feedback structure PDO topology and relevant damping losses (ρ=0.005). a) is the result for δ=1, and b) is for δ=-1.

Figure 6. Upper view and schematic of the PDO circuit used in the measurements.

Figure 7. Oscilloscope screen captures of resonator position (1), MEMS input pulses (2), delayed comparator output (D2,D1) and sample clock (D0), for $f_S=4f_0$ for single (a) and double (b) feedback structures (δ=1).

Figure 8. Oscilloscope screen captures of resonator position (1), MEMS input pulses (2), delayed comparator output (D2,D1) and sample clock (D0), and $f_S=2{,}489f_0$ for double feedback structures with δ=1 (a) and with δ=-1 (b).

Figure 9. Analog position (a) and bit stream (b) spectra for a δ=1 double feedback structure under the same experimental conditions as in Figure 8.a. Analog position (c) and bit stream (d) spectra for a δ=-1 double feedback structure under the same experimental conditions as in Figure 8.b.

Figure 10. Oscilloscope screen captures of resonator position (1), MEMS input pulses (2), delayed comparator output (D1) and sample clock (D0), and $f_S=1{,}23f_0$ for double feedback structures with δ=1 (a) and with δ=-1 (b).

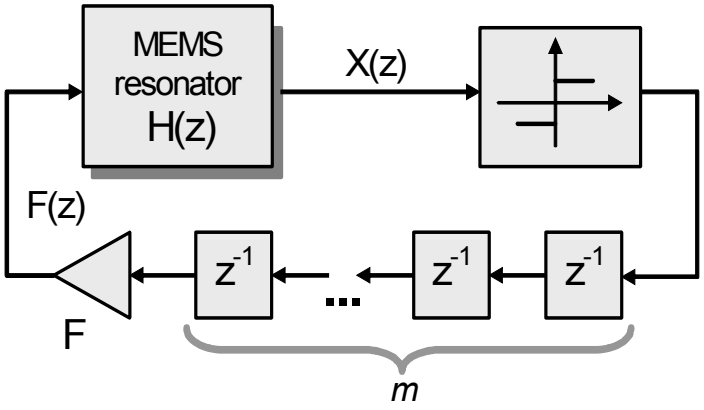

Figure 1

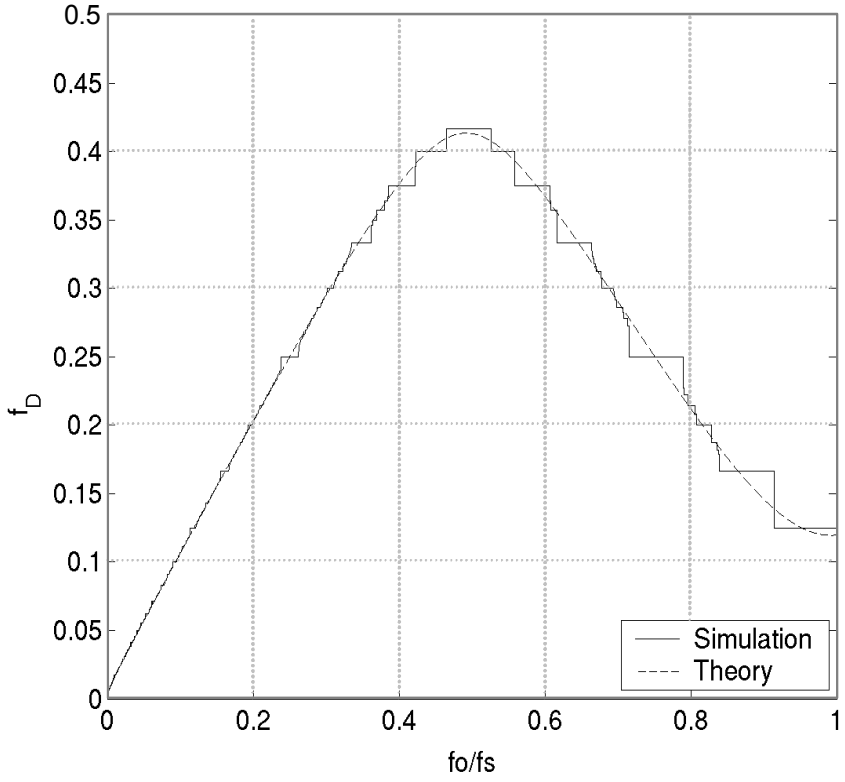

Figure 2

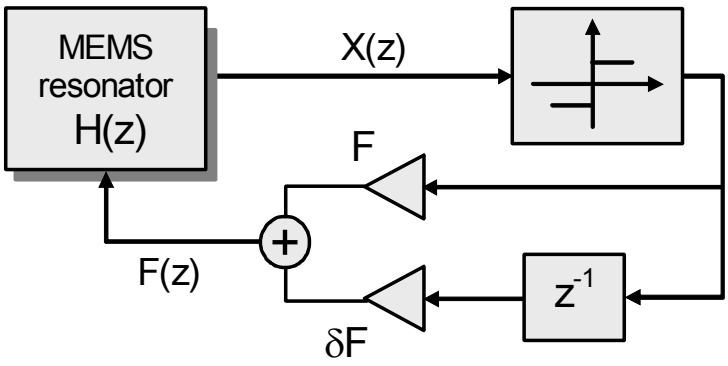

Figure 3

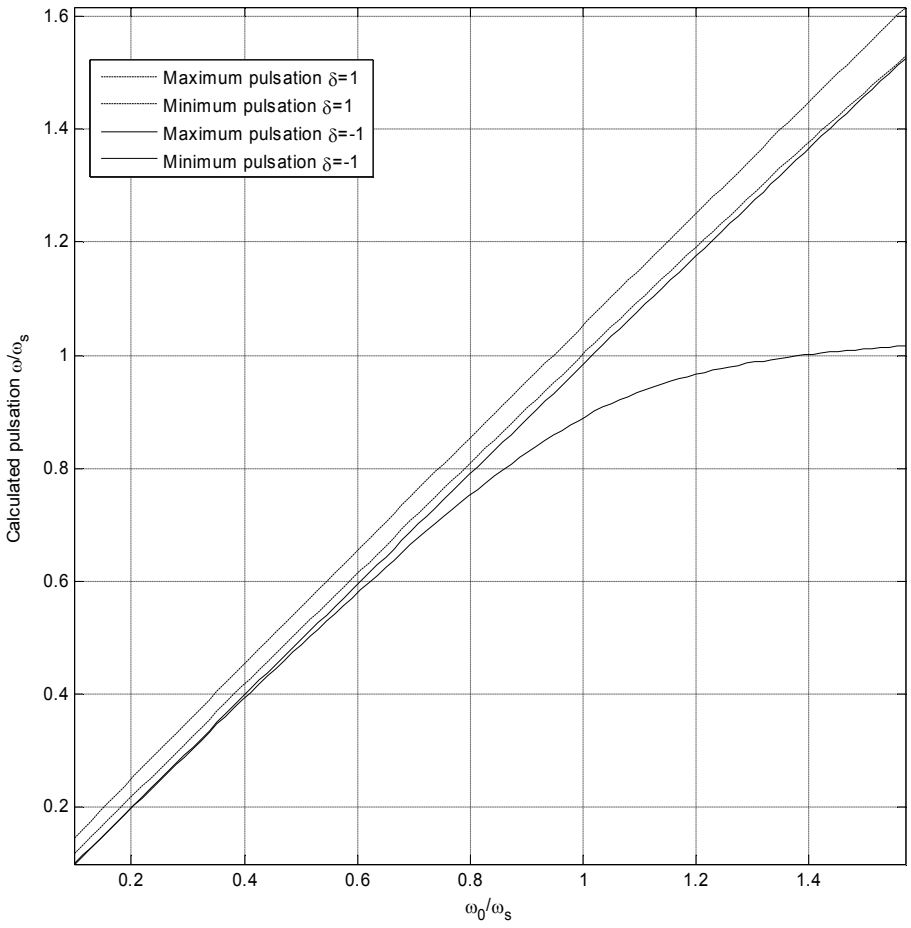
Maximum pulsation δ=1
Minimum pulsation δ=1
Maximum pulsation δ=-1
Minimum pulsation δ=-1
Calculated pulsation ω/ωs
ω0/ωs
1.6
1.4
1.2
1
0.8
0.6
0.4
0.2
0.2
0.4
0.6
0.8
1
1.2
1.4

Figure 4

a)

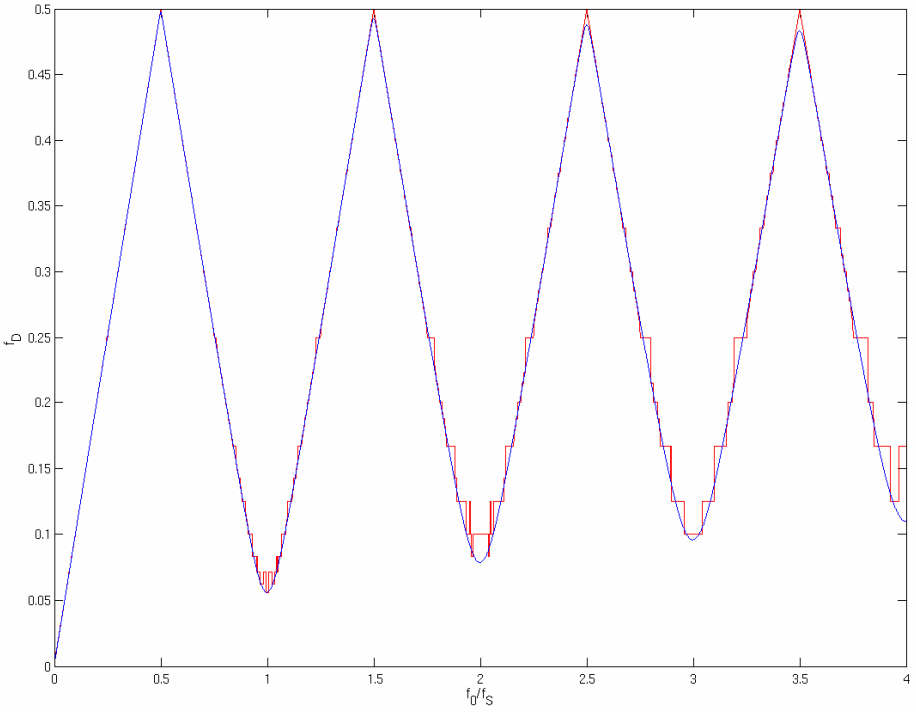
0.5
0.45
0.4
0.35
0.3
0.25
0.2
0.15
0.1
0.05
0
f_D
0
0.5
1
1.5
2
2.5
3
3.5
4
f_O/f_S

b)

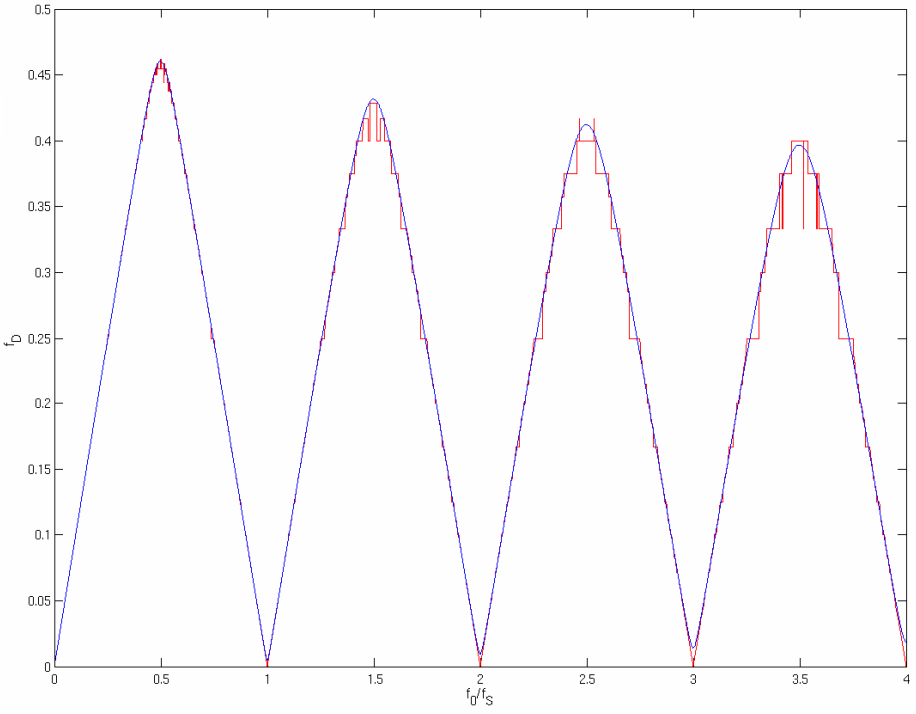
0.5
0.45
0.4
0.35
0.3
0.25
0.2
0.15
0.1
0.05
0
f_D
0
0.5
1
1.5
2
2.5
3
3.5
4
f_O/f_S

Figure 5

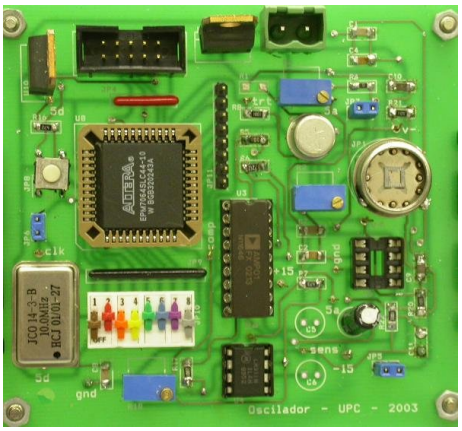
Oscilador - UPC - 2003

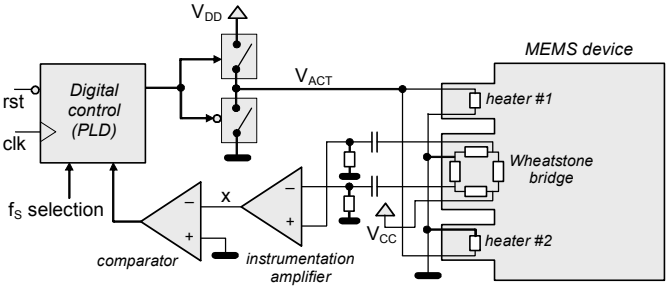
V_DD
MEMS device
V_ACT
rst
clk
Digital control (PLD)
heater #1
Wheatstone bridge
f_S selection
x
V_CC
heater #2
comparator
instrumentation amplifier

Figure 6

a)

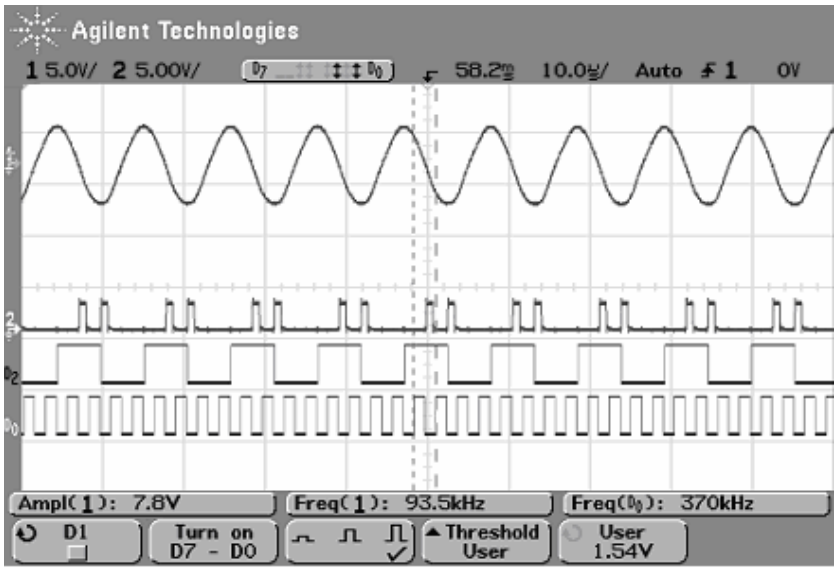
Agilent Technologies
1 5.0V/ 2 5.00V/
58.2ms
10.0s/
Auto
1
0V
Ampl(1): 7.8V
Freq(1): 93.5kHz
Freq(D0): 370kHz
D1
Turn on D7 - D0
Threshold User
User 1.54V

b)

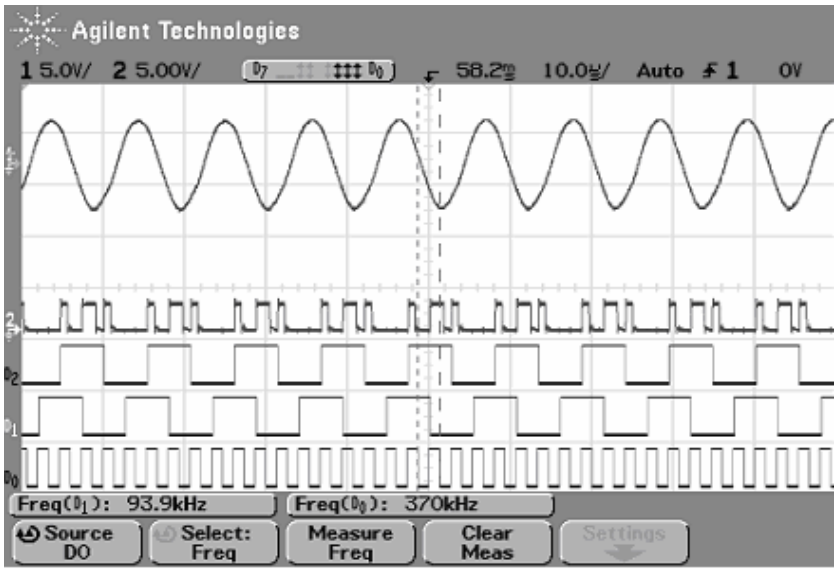
Agilent Technologies
1 5.0V/ 2 5.00V/
58.2ms 10.0s/ Auto 1 0V
Freq(D1): 93.9kHz
Freq(D0): 370kHz
Source D0
Select: Freq
Measure Freq
Clear Meas
Settings

Figure 7

a)

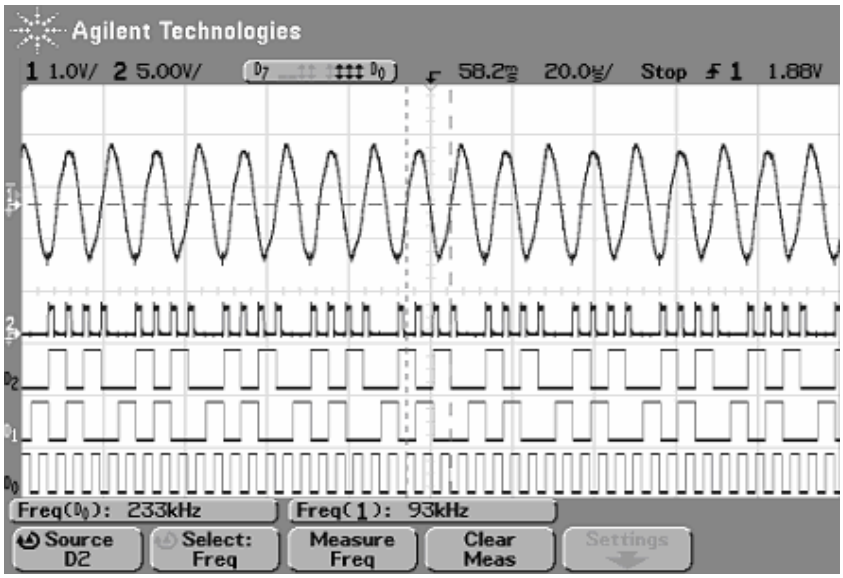
Agilent Technologies
1 1.0V/ 2 5.00V/
58.2ms 20.0ms/ Stop 1 1.88V
Freq(D0): 233kHz
Freq(1): 93kHz
Source D2
Select: Freq
Measure Freq
Clear Meas
Settings

b)

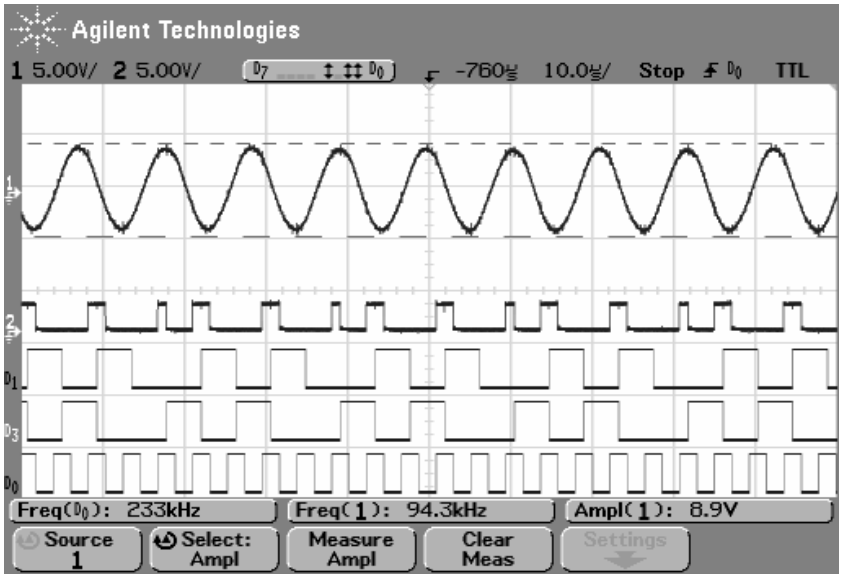
Agilent Technologies
1 5.00V/ 2 5.00V/
-760ns 10.0ns/ Stop D0 TTL
Freq(D0): 233kHz
Freq(1): 94.3kHz
Ampl(1): 8.9V
Source 1
Select: Ampl
Measure Ampl
Clear Meas
Settings

Figure 8

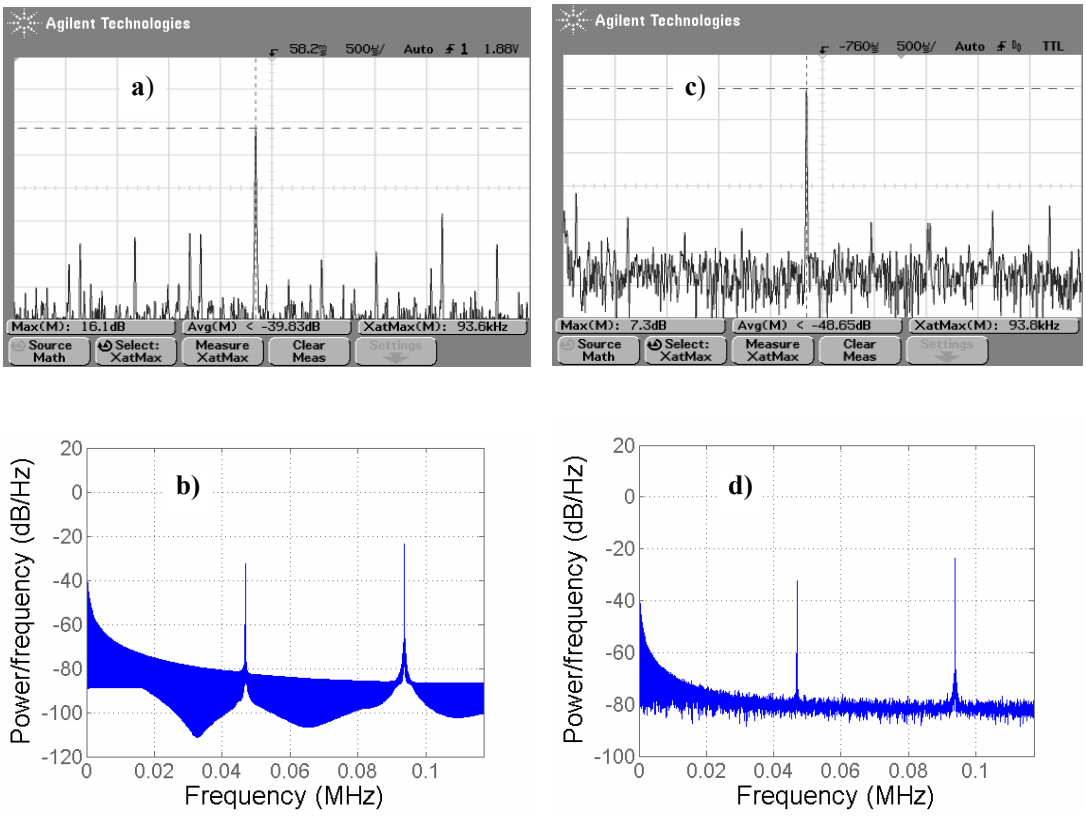
Agilent Technologies
a)
Max(M): 16.1dB
Avg(M) < -39.83dB
XatMax(M): 93.6kHz
Source Math
Select: XatMax
Measure XatMax
Clear Meas
Settings
Agilent Technologies
c)
Max(M): 7.3dB
Avg(M) < -48.65dB
XatMax(M): 93.8kHz
Source Math
Select: XatMax
Measure XatMax
Clear Meas
Settings
b)
Power/frequency (dB/Hz)
Frequency (MHz)
d)
Power/frequency (dB/Hz)
Frequency (MHz)

Figure 9

a)

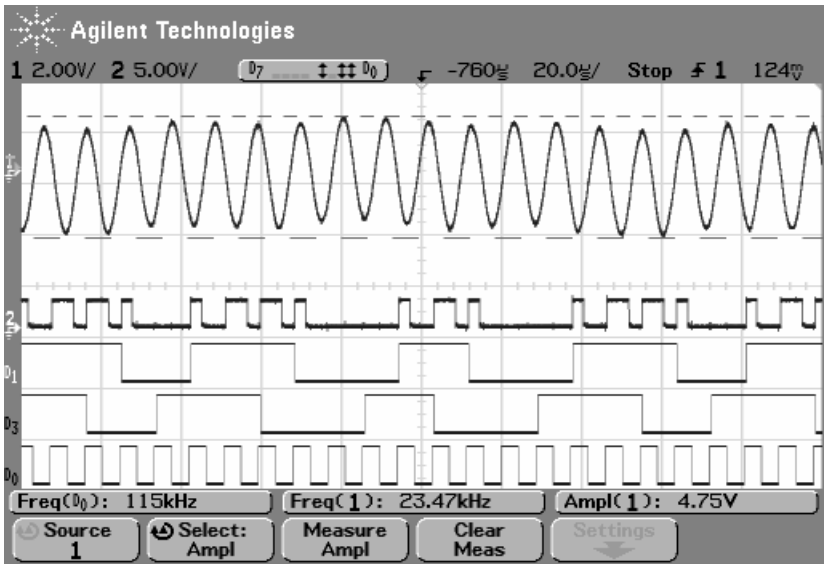
Agilent Technologies
1 2.00V/ 2 5.00V/
-760
20.0/
Stop
1
Freq(D0): 115kHz
Freq(1): 23.47kHz
Ampl(1): 4.75V
Source 1
Select: Ampl
Measure Ampl
Clear Meas
Settings

b)

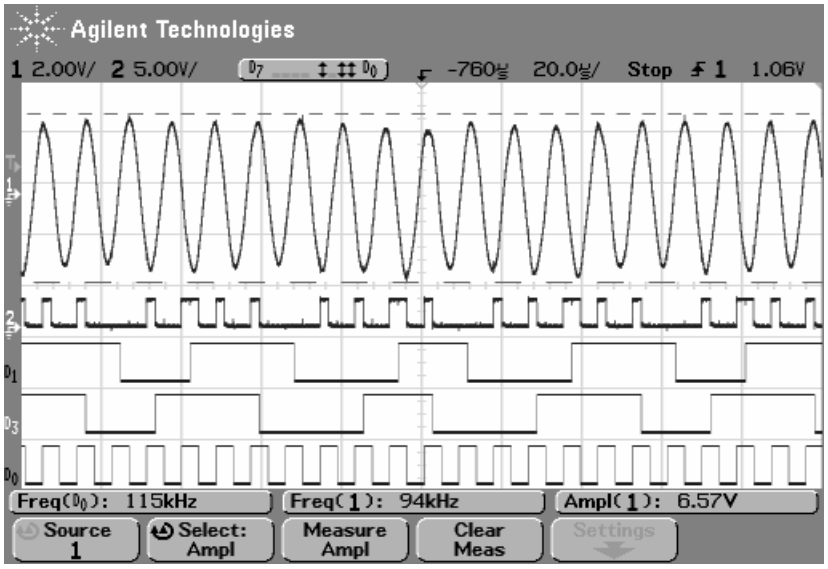
Agilent Technologies
1 2.00V/ 2 5.00V/
-760
20.0/
Stop
1
1.06V
Freq(D0): 115kHz
Freq(1): 94kHz
Ampl(1): 6.57V
Source 1
Select: Ampl
Measure Ampl
Clear Meas
Settings

Figure 10